Chinese Chemical Letters 36 (2025) 109751

Contents lists available at ScienceDirect

Chinese Chemical Letters

journal homepage: www.elsevier.com/locate/cclet

Encapsulating lipase on the surface of magnetic ZIF-8 nanosphers with mesoporous SiO_2 nano-membrane for enhancing catalytic performance

Guang-Xu Duan[a,1], Queting Chen[d,1], Rui-Rui Shao[a], Hui-Huang Sun[a], Tong Yuan[a], Dong-Hao Zhang[a,b,c,*]

[a] College of Pharmaceutical Science, Hebei University, Baoding 071002, China
[b] Key Laboratory of Pharmaceutical Quality Control of Hebei Province, College of Pharmaceutical Science, Hebei University, Baoding 071002, China
[c] Institute of Life Science and Green Development, Hebei University, Baoding 071002, China
[d] Affiliated Hospital of Hebei University, Baoding 071000, China

ARTICLE INFO

Article history:
Received 11 January 2024
Revised 1 March 2024
Accepted 6 March 2024
Available online 8 March 2024

Keywords:
Enzyme immobilization
ZIF-8
Encapsulation
Mesoporous silica membrane
Lipase activity

ABSTRACT

The preparation of immobilized enzyme with excellent performance is one of the difficulties that restrict the application of enzyme catalysis technology. Here, *Candida rugosa* lipase (CRL) was firstly adsorbed on the surface of magnetic zeolitic imidazolate framework-8 (ZIF-8) nanospheres, which was further encapsulated with a mesoporous SiO_2 nano-membrane formed by tetraethyl orthosilicate (TEOS) polycondensation. Consequently, lipase could be firmly immobilized on carrier surface by physical binding rather than chemical binding, which did not damage the active conformation of enzyme. There were mesopores on the silica nano-membrane, which could improve the accessibility of enzyme and its apparent catalytic activity. Moreover, silica membrane encapsulation could also improve the stability of enzyme, suggesting an effective enzyme immobilization strategy. It showed that TEOS amount and the encapsulation time had significant effects on the thickness of silica membrane and the enzyme activity. The analysis in enzyme activity and protein secondary structure showed that lipase encapsulated in silica membrane retained the active conformation to the greatest extent. Compared with the adsorbed lipase, the encapsulated lipase increased its thermostability by 3 times and resistance to chemical denaturants by 7 times. The relative enzyme activity remained around 80% after 8 repetitions, while the adsorbed lipase only remained at 7.3%.

Enzymes have been widely used in biopharmaceuticals, food processing, fine chemicals, biofuels and other fields [1–3]. However, enzymes are susceptible to inactivation due to the factors such as temperature and pH, and are difficult to recycle and continuously produce [4]. Immobilization of enzymes can not only improve their stability and reduce enzyme inactivation, but also improve their reuse efficiency. The traditional methods of enzyme immobilization include adsorption [5], embedding [6], covalent bonding [7,8] and cross-linking [9,10]. Adsorption has little damage to the active conformation of enzyme, but the adsorbed enzyme is prone to detachment from support. Embedding enzyme into the interior of polymer network structure can firmly immobilize enzyme molecules and retain its structure, but the mass transfer resistance of substrate entering into the support is large, reducing the apparent activity of enzyme [11,12]. The covalent method can firmly immobilize enzyme on the surface of support and reduce the mass transfer resistance, but the violent reaction is easy to destroy enzyme conformation and decrease its activity [13]. In response to the drawbacks of traditional methods, many new support materials [14–16] and new immobilization strategies have continuously emerged [17,18]. Among these materials, metal organic framework (MOF) and magnetic MOF nanopheres have many advantages [19,20], such as super-paramagnetism, large surface area, and surface hydrophobicity, which facilitates the magnetic separation, high enzyme loading and lipase activation.

This study used a silica membrane with mesoporous structure to encapsulate enzyme molecules adsorbed on the surface of support, which combined the advantages of adsorption and embedding. This immobilization strategy could not only solve the problems of enzyme leakage and substrate mass transfer, but also retain the catalytic activity of enzyme by preventing enzyme from chemical reaction. Besides, the encapsulation with silica membrane could protect the active conformation of enzyme and make

* Corresponding author.
E-mail addresses: donghaozhang1@163.com, dhzhang@hbu.edu.cn (D.-H. Zhang).
[1] These authors contributed equally to this work.

https://doi.org/10.1016/j.cclet.2024.109751
1001-8417/

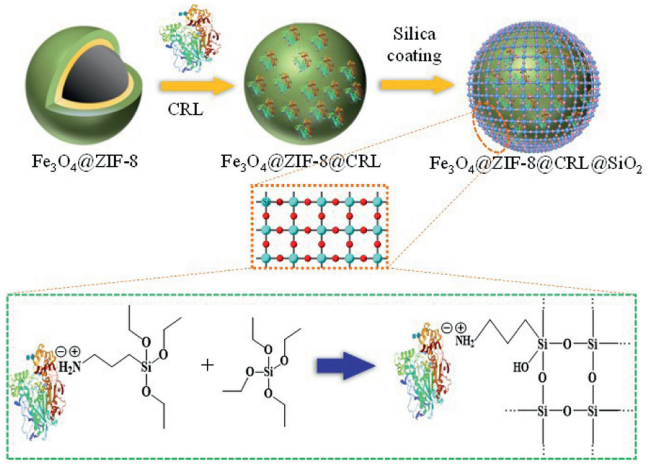

Fig. 1. Scheme of lipase encapsulated by silica nano-membrane on the surface of magnetic ZIF-8.

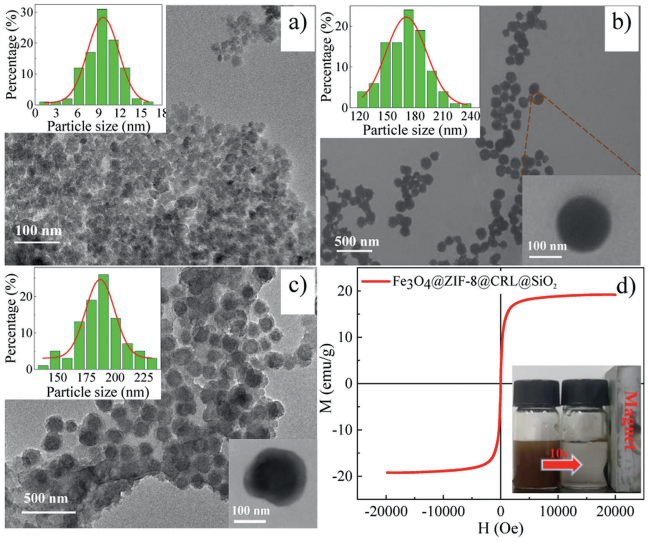

Fig. 2. TEM image and the particle size distribution of (a) Fe_3O_4, (b) Fe_3O_4@ZIF-8 and (c) Fe_3O_4@ZIF-8@CRL@SiO_2. (d) Vibrating sample magnetic strength (VSM) of Fe_3O_4@ZIF-8@CRL@SiO_2.

it more stable. We first prepared zeolitic imidazolate framework-8 (ZIF-8) magnetic nanospheres and adsorbed lipase onto the surface of nanospheres, and then coated a SiO_2 nano-membrane with mesopores on the surface of nanospheres by hydrolyzing and condensing. Consequently, lipase was encapsulated on the surface of nanospheres, as shown in Fig. 1.

Fig. 2a shows the morphology of Fe_3O_4 magnetic particles observed under transmission electron microscopy (TEM), and their particle sizes are statistically analyzed. It can be seen that the resulting Fe_3O_4 magnetic particles have good monodispersity (particle dispersity index (PDI) = 0.381), with a concentrated particle size distribution at 9.5 nm. Fig. 2b shows the TEM morphology and particle size distribution of Fe_3O_4@ZIF-8 magnetic nanospheres. As observed, the size of magnetic particles significantly increases after being coated with ZIF-8, and Fe_3O_4@ZIF-8 is spherical and has good dispersibility (PDI = 0.302), with a concentrated particle size distribution at 176.8 nm. Fig. 2c shows the morphology and particle size distribution of the immobilized lipase with silica membrane encapsulation (Fe_3O_4@ZIF-8@CRL@SiO_2; CRL, *Candida rugosa* lipase). It can be seen that after adsorbing lipase on Fe_3O_4@ZIF-8 and subsequently encapsulating it with SiO_2 nano-membrane,

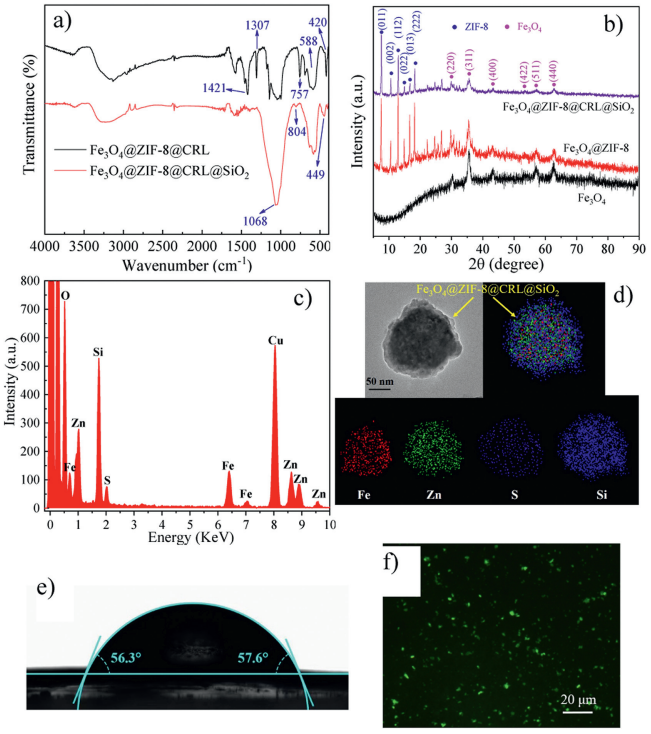

Fig. 3. (a) Infrared spectra of Fe_3O_4@ZIF-8@CRL and Fe_3O_4@ZIF-8@CRL@SiO_2. (b) XRD of Fe_3O_4, Fe_3O_4@ZIF-8 and Fe_3O_4@ZIF-8@CRL@SiO_2. (c) EDS, (d) TEM mapping, (e) water contact angle, and (f) fluorescence characterization of Fe_3O_4@ZIF-8@CRL@SiO_2.

the particle size of magnetic nanospheres further increases to 190.1 nm, indicating the successful coating with a nano-thickness silica membrane. Fig. 2d shows the hysteresis curve of Fe_3O_4@ZIF-8@CRL@SiO_2, displaying typical superparamagnetism with a saturation magnetization of 19.18 emu/g. As seen from the insert, Fe_3O_4@ZIF-8@CRL@SiO_2 has good dispersibility in aqueous solution and can achieve rapid and effective separation under magnetic field.

In order to effectively form the SiO_2 membrane on nanospheres by tetraethyl orthosilicate (TEOS) polymerization, 3-aminopropyltriethoxysilane (APTES) was adsorbed on Fe_3O_4@ZIF-8@CRL in advance before adding TEOS by the electrostatic interaction between the positively charged amino group of APTES and the negatively charged lipase (pI = 4.4). Fig. 3a shows the infrared absorption spectra of Fe_3O_4@ZIF-8@CRL and Fe_3O_4@ZIF-8@CRL@SiO_2. In the spectrum of Fe_3O_4@ZIF-8@CRL, the peaks at 588 and 420 cm^{-1} respectively correspond to the stretching vibration absorptions of the Fe-O bond and Zn-N bond, the sharp peaks at 757 and 1307 cm^{-1} belong to the bending vibration peak of imidazole ring in ZIF-8, and the peaks at 1421 and 1456 cm^{-1} belong to the stretching vibration peaks of imidazole ring. In the spectrum of Fe_3O_4@ZIF-8@CRL@SiO_2, a strong and wide anti symmetric stretching vibration absorption peak of Si-O-Si appears at 1068 cm^{-1}. Moreover, a symmetric stretching vibration absorption peak of Si-O bond appears at 804 cm^{-1}, and a bending vibration absorption peak of Si-O bond appears around 449 cm^{-1}. These peaks imply the success of SiO_2 nano-membrane coating.

Fig. 3b shows the X-ray diffraction (XRD) images of Fe_3O_4 (black curve), Fe_3O_4@ZIF-8 (red curve) and Fe_3O_4@ZIF-8@CRL@SiO_2 (purple curve). The black curve exhibits characteristic peaks of Fe_3O_4 particles at 30.2°, 35.4°, 43.1°, 53.7°, 57.1° and 62.8°, corresponding to the diffraction crystal planes of Fe_3O_4 at (220), (311), (400), (422), (511) and (440), respectively. In the red curve, it appears

the characteristic peaks of ZIF-8 at 7.4°, 10.5°, 12.9°, 14.8°, 16.6° and 18.1°, corresponding to the diffraction crystal planes of ZIF-8 at (011), (002), (112), (022), (013), and (222), respectively. In the purple curve, no obvious SiO_2 characteristic peaks appear because of the amorphous structure of silica membrane. But compared with the curves of Fe_3O_4 and Fe_3O_4@ZIF-8, it can be seen that the diffraction peak intensity of ZIF-8 and Fe_3O_4 in Fe_3O_4@ZIF-8@CRL@SiO_2 is greatly cut down due to SiO_2 coating.

The energy dispersive spectrum (EDS) and TEM mapping of Fe_3O_4@ZIF-8@CRL@SiO_2 are shown in Figs. 3c and d, respectively. In Fig. 3c, The EDS spectrum analysis shows that the main components of immobilized lipase are Fe, Zn, S and Si, wherein Fe and O are from Fe_3O_4, Zn is from ZIF-8, S is from the cysteine residues of lipase, Si is from SiO_2 membrane, and Cu is from the copper mesh used for TEM. From the TEM mapping scan of Fe_3O_4@ZIF-8@CRL@SiO_2 in Fig. 3d, it can be seen that the elements distribution order is Fe, Zn, S, and Si from the inside out. It can also be seen that the immobilized lipase is spherical in shape, and Fe element is distributed inside the central area, indicating that Fe_3O_4 nano particles are located at the core of nanospheres. There is a distribution of Zn element outside the Fe element, indicating the coat of ZIF-8 outside Fe_3O_4 nano particles. The content of S element is rich and evenly distributed on the surface of nanospheres, suggesting that a large number of lipase molecules are immobilized on the nanospheres. The TEM mapping results also showed that Si element is uniformly distributed on the surface of nanospheres, further confirming the coating of SiO_2.

In general, the surface of enzyme molecules is bound to a certain number of water molecules referred to as the "essential hydration layer", which is necessary for the enzyme to maintain its activity [21,22]. Besides, CRL is a special enzyme with interfacial activity, and a hydrophobic interface facilitates the opening of the "active lid" and activates the catalytic activity of lipase [23]. After immobilizing lipase onto the carrier, the hydrophobic carrier surface will affect the "hydration layer" of lipase and its activity; On the other hand, the hydrophobic carrier surface can also affect the opening and closing of lipase's "active lid". Fig. 3e shows the hydrophilicity of immobilized enzyme. As can be seen, the contact angle is about 57°, indicating that the surface of Fe_3O_4@ZIF-8@CRL@SiO_2 has good hydrophilicity. Besides, the water contact angle of Fe_3O_4@ZIF-8 is greater than 90° as shown in Fig. S1 (Supporting information), indicating a hydrophobic surface. Due to the fact that the one end of lipase is in contact with hydrophobic ZIF-8 [24] and the other end is in contact with hydrophilic SiO_2, this amphiphilic carrier can not only improve enzyme activity by maintaining the "hydration layer", but also activate lipase activity by opening the lid of lipase.

Fe_3O_4@ZIF-8@CRL@SiO_2 was prepared using fluorescence labeling lipase and further observed under a fluorescence microscope. As can be seen from Fig. 3f, the surface of nanospheres emitted strong green fluorescence, indicating the successful immobilization of lipase on nanospheres.

On the surface of Fe_3O_4@ZIF-8@CRL@SiO_2, there are many pore structures in the SiO_2 nano-membrane. In order to evaluate the pore size, the changes in specific surface area and pore size distribution were obtained by comparing the nitrogen adsorption/desorption isotherm of Fe_3O_4@ZIF-8 before and after silica membrane encapsulation (Fig. S2 in Supporting information). In Fig. S2a, The specific surface area of Fe_3O_4@ZIF-8 is 436.4 m^2/g. There is no hysteresis loop in the isotherm curve, indicating that there is no mesoporous structure on the surface of Fe_3O_4@ZIF-8. In Fig. S2b, the specific surface area of Fe_3O_4@ZIF-8@CRL@SiO_2 is 216.2 m^2/g, which is smaller than that of Fe_3O_4@ZIF-8 because of the larger particle size. Particularly, there is a significant hysteresis loop in Fig. S2b, indicating the presence of layered structures including crack pores on the surface of nanospheres. This result confirms that there are numerous mesoporous structures on the surface of Fe_3O_4@ZIF-8@CRL@SiO_2, with pore sizes concentrated at 3.9 nm as shown in Fig. S2b. To be satisfactory, the pore size of silica membrane (3.9 nm) is smaller than the size of CRL lipase molecule ($5.0 \times 4.2 \times 3.3$ nm^3) [25,26], suggesting that mesoporous silica membrane can firmly lock lipase molecules on the surface of Fe_3O_4@ZIF-8 and prevent them from falling off. Moreover, the mesopores on SiO_2 nano-membrane is beneficial for improving the accessibility of lipase, and thus improving the apparent activity of immobilized enzyme.

To study whether substrate molecules can smoothly diffuse through the mesoporous structures (3.9 nm), we simulated the process of ethanol/palmitic acid diffusion through the mesopores of silica membrane using lipase-catalyzed esterification of palmitic acid with ethanol. Fig. S3a (Supporting information) shows the diffusion results of ethanol/palmitic acid in the longitudinal direction inside the pores at different time (0, 0.5, 1, 3, 4, 5 ns). It can be seen that there is no significant diffusion of ethanol and palmitic acid at 0.1 ns. As time goes on to 5 ns, ethanol and palmitic acid have diffused into the pores. Fig. S3b (Supporting information) shows the diffusion results of ethanol/palmitic acid in the lateral direction inside the pores. At 0 ns, it can be seen that ethanol and palmitic acid are located on the surface of pores and have not yet diffused into the pores. At 5 ns, ethanol and palmitic acid have significantly shifted towards the interior of pores. The simulation results show that the diffusion rate of substrate molecules is fast, indicating small mass transfer resistance. Therefore, the SiO_2 nano-membrane does not affect the contact of enzyme with substrates, which helps to improve the apparent catalytic activity of immobilized enzyme.

Fig. S4a (Supporting information) shows the thermogravimetric curve (TGA) of Fe_3O_4, Fe_3O_4@ZIF-8, Fe_3O_4@ZIF-8@CRL and Fe_3O_4@ZIF-8@CRL@SiO_2. As observed, the total weight loss ratio of Fe_3O_4 nanoparticles modified with sodium citrate is 27.28%, including water loss and sodium citrate decomposition. The total weight loss ratio of Fe_3O_4@ZIF-8 magnetic nanospheres is 47.49%. And the reason for rapid weight loss above 580 °C is due to the decomposition of imidazole bridges in the metal-organic framework, which results in the collapse of crystal structure [27]. The total weight loss ratio of Fe_3O_4@ZIF-8@CRL is 50.66%. The lipase molecules adsorbed on the surface of nanospheres decomposes at high temperature, resulting in a higher weight loss ratio than Fe_3O_4@ZIF-8. And the difference value in total weight loss ratio (3.17%) between Fe_3O_4@ZIF-8 and Fe_3O_4@ZIF-8@CRL is due to the enzyme loading, which is roughly consistent with the enzyme loading (36.48 mg/g) determined by measuring the enzyme concentration changes in the supernatant before and after enzyme immobilization. Besides, the total weight loss ratio of Fe_3O_4@ZIF-8@CRL@SiO_2 is 49.08%.

To investigate the binding strength between enzyme and carrier, Fe_3O_4@ZIF-8@CRL and Fe_3O_4@ZIF-8@CRL@SiO_2 were eluted/desorbed with a high concentration salt solution, and the results were compared in Fig. S4b (Supporting information). It can be seen that after elution treatment with 1.5 mol/L NaCl, the enzyme loading amount of Fe_3O_4@ZIF-8@CRL has significantly decreased with a desorption ratio of 67.8%, while the enzyme loading amount of Fe_3O_4@ZIF-8@CRL@SiO_2 only has a little change with a desorption ratio of 9.0%. In Fe_3O_4@ZIF-8@CRL, the binding between lipase and carrier relies on weak physical adsorption. At high ionic strength, the non-covalent binding is destroyed, causing a large amount of enzyme leakage. In Fe_3O_4@ZIF-8@CRL@SiO_2, lipase is encapsulated on Fe_3O_4@ZIF-8 by silica nano-membrane. Therefore, the enzyme molecules can be immobilized firmly and are not prone to leakage.

Due to the complex interaction between enzyme and carrier, the immobilization process will inevitably destroy the structure of enzyme in part or even in whole. One of the purposes in this

work is to maintain the active conformation of lipase during immobilization. It is generally believed that physical immobilization is beneficial for preserving the natural conformation of enzyme. Here, the physical encapsulation is used to firmly immobilize lipase on the surface of carrier, avoiding enzyme inactivity caused by covalent immobilization. Therefore, it is necessary to evaluate the activity and conformation of lipase after immobilization. Fig. S4c (Supporting information) compares the activities of free lipase with Fe_3O_4@ZIF-8@CRL and Fe_3O_4@ZIF-8@CRL@SiO_2. It can be seen that after adsorbing lipase on Fe_3O_4@ZIF-8, there is a increase in enzyme activity from 46.0 U/mg to 57.8 U/mg, indicating that the hydrophobic ZIF-8 can activate lipase [28,29]. Moreover, the activity of Fe_3O_4@ZIF-8@CRL@SiO_2 is further improved compared with Fe_3O_4@ZIF-8@CRL, which may be attributed to that the hydrophilicity of silica membrane helps to maintain the "essential hydration layer" of enzyme and open the "active lid".

Infrared spectroscopy is an effective tool for analyzing the structure of proteins [30–32]. The changes in the absorption bands of protein secondary structures at 1700–1600 cm^{-1} (amide I band) are very sensitive, making it the most meaningful band for analyzing secondary structure changes [33–35]. Fig. S5a (Supporting information) shows the absorption spectra of free lipase, Fe_3O_4@ZIF-8@CRL, and Fe_3O_4@ZIF-8@CRL@SiO_2 in amide I band. The dark blue curve shows the infrared spectra of lipase at 1700–1600 cm^{-1}, which can be decomposed into multiple sub-peaks of secondary structures. The sub-peaks at 1610–1640 cm^{-1} and 1680–1700 cm^{-1} are assigned to β-sheet (pink), the sub-peaks at 1640–1650 cm^{-1} are assigned to random coil (light blue), the sub-peaks at 1650–1660 cm^{-1} are assigned to α-helix (green), and the sub-peaks at 1660–1680 cm^{-1} are assigned to β-turn (yellow) [36]. The content of each secondary structure in protein can be calculated based on the sub-peak area (Fig. S5b in Supporting information). As can be seen, the contents of α-helix and β-sheet both increase after adsorbing lipase on Fe_3O_4@ZIF-8. Moreover, after encapsulating Fe_3O_4@ZIF-8@CRL into silica membrane, the contents of α-helix and β-sheet further increase. Compared Fe_3O_4@ZIF-8@CRL@SiO_2 with free lipase, the contents of α-helix and β-sheet increase, and the contents of β-turn and random coil decrease, indicating the increase in rigidity and stability of lipase conformation.

The change in the added amount of TEOS may change the thickness of silica membrane on Fe_3O_4@ZIF-8@CRL@SiO_2, thereby affecting the stability and apparent activity of the immobilized enzyme. Figs. S6a–d (Supporting information) show the TEM images of Fe_3O_4@ZIF-8@CRL@SiO_2 prepared respectively by adding different amount of TEOS. As can be seen, the adding amount of TEOS has significant effect on the thickness of silica membrane formed on the surface of nanospheres, and the thickness of silica membrane gradually increases with the increase of TEOS. When TEOS amount is 22.4 μL, the thickness of silica membrane is 11 nm. While the thickness reaches 49 nm with 100.8 μL TEOS. In order to encapsulate lipase on the surface of nanospheres, a certain amount of TEOS need to be added to form a thin layer of silica membrane. On the other hand, the increase in the thickness of silica membrane may decrease the accessibility of enzyme, thereby affecting the apparent activity of immobilized enzyme.

Fig. S6e (Supporting information) shows the effect of the thickness of silica membrane on lipase encapsulation. It can be seen that with 11.2 μL TEOS, the lipase on Fe_3O_4@ZIF-8@CRL@SiO_2 is prone to detachment when dealing with high salt solution, resulting in 59.6% of enzyme leakage. When 22.4 μL TEOS is added, only 9.0% of lipase on Fe_3O_4@ZIF-8@CRL@SiO_2 leaked, indicating that lipase can be effectively encapsulated only when the formed silica membrane reaches a certain thickness. Fig. S6f (Supporting information) shows the effect of TEOS amount on the enzyme specific activity and enzyme loading of Fe_3O_4@ZIF-8@CRL@SiO_2. As can be seen, when TEOS amount increases from 11.2 μL to 22.4 μL, lipase activity slightly increases from 51.0 U/mg to 57.8 U/mg. But when TEOS continues to increase, the activity rapidly decreases to 5.5 U/mg at 100.8 μL. These results suggest that the adding amount of TEOS should be appropriate to achieve the optimum encapsulation. An increase in silica membrane thickness will increase the mass transfer resistance of substrates/products and thus result in a decrease in the apparent activity of enzyme. Besides, it can also be seen that TEOS amount has little effect on lipase loading.

We further determined the enzymatic kinetic parameters of Fe_3O_4@ZIF-8@CRL@SiO_2. Fig. S7 (Supporting information) shows the Lineweaver-Burk plot of free lipase and the encapsulated lipase. The Michaelis constant (K_m) and maximum reaction rate (V_{max}) have been calculated and listed in Table S1 (Supporting information). The K_{cat}/K_m value of Fe_3O_4@ZIF-8@CRL@SiO_2 is higher than that of free lipase, indicating a high catalytic efficiency of Fe_3O_4@ZIF-8@CRL@SiO_2. It can be ascribed to the hydrophobic interaction between ZIF-8 and the lid of lipase, resulting in interfacial activation [37,38].

The stability of immobilized enzyme is of great significance in industrial operations. The thermal stabilities of free lipase, Fe_3O_4@ZIF-8@CRL and Fe_3O_4@ZIF-8@CRL@SiO_2 are shown in Fig. 4a. After 3 h of incubation at 45 °C, the activity of free lipase decreases to only about 40% of the initial activity, indicating a low thermostability. Even after adsorbing lipase on Fe_3O_4@ZIF-8 to obtain Fe_3O_4@ZIF-8@CRL, the residual activity only increases by 10% and reaches 50% of the initial activity after 3 h of incubation. However, after encapsulating lipase into silica membrane, the residual activity has significantly increased to about 90% after 3 h of incubation, indicating a good thermostability of Fe_3O_4@ZIF-8@CRL@SiO_2. Besides, after 5 h of incubation, free lipase almost completely loses its activity and Fe_3O_4@ZIF-8@CRL remained 24% of its initial activity, while Fe_3O_4@ZIF-8@CRL@SiO_2 retain up to 75% of its initial activity. These results indicate that encapsulating enzyme into silica membrane is beneficial for improving the thermal stability of enzyme. It can be attributed to that the external silica membrane confines enzyme molecules within a limited space and prevents the unfolding and denaturation of enzyme at high temperature, which effectively inhibits enzyme inactivation.

Fig. 4b evaluates the tolerance of Fe_3O_4@ZIF-8@CRL@SiO_2 to chemical denaturants. After 30 min treatment with 6 mol/L urea, the relative residual activities of free lipase, Fe_3O_4@ZIF-8@CRL, and Fe_3O_4@ZIF-8@CRL@SiO_2 are respectively 9.3%, 31.4% and 67.0%. Furthermore, after 30 min treatment with 0.2% sodium dodecyl sulfate (SDS), the relative residual activities of free lipase, Fe_3O_4@ZIF-8@CRL, and Fe_3O_4@ZIF-8@CRL@SiO_2 are respectively 12.2%, 30.4% and 54.4%. These results demonstrate that Fe_3O_4@ZIF-8@CRL@SiO_2 has good resistance to denaturants, indicating that silica membrane encapsulation reduces the damage of denaturants to enzyme conformation and provides protection for the enzyme. Fig. 4c further compares their storage stability. After 20 days of storage at room temperature, the relative activities of free lipase and Fe_3O_4@ZIF-8@CRL respectively decrease to about 5% and 9%, while Fe_3O_4@ZIF-8@CRL@SiO_2 can still remain 60% of its initial activity. This once again confirms that Fe_3O_4@ZIF-8@CRL@SiO_2 has high stability.

Fig. 4d shows the reusability of Fe_3O_4@ZIF-8@CRL and Fe_3O_4@ZIF-8@CRL@SiO_2. After 8 recycles, Fe_3O_4@ZIF-8@CRL only retains 7.3% of its initial activity, while Fe_3O_4@ZIF-8@CRL@SiO_2 retains about 80% of its initial activity. This poor reusability of Fe_3O_4@ZIF-8@CRL is due to the weak non-covalent interaction between enzyme and carrier, which leads to the serious leakage of enzyme from carrier during use and a decrease in enzyme activity. To our satisfaction, Fe_3O_4@ZIF-8@CRL@SiO_2 can firmly encapsulate lipase in SiO_2 nano-membrane, thereby improving the reusability.

In summary, Fe_3O_4@ZIF-8@CRL@SiO_2 is prepared by encapsulating enzymes in mesoporous SiO_2 nano-membrane. Compared with

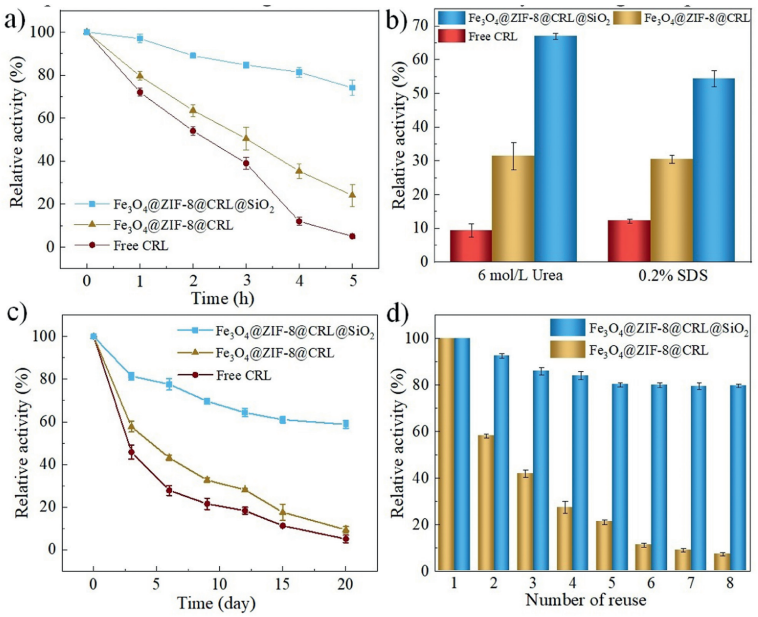

Fig. 4. (a) Thermal stability at 45 °C, (b) tolerance to denaturants, and (c) storage stability in buffer at room temperature of Fe_3O_4@ZIF-8@CRL@SiO_2, Fe_3O_4@ZIF-8@CRL and free lipase. (d) Reusability of Fe_3O_4@ZIF-8@CRL@SiO_2 and Fe_3O_4@ZIF-8@CRL. The error bar means the standard deviation (SD) ($n = 5$).

the traditional immobilized methods, silica membrane encapsulation can immobilize enzyme firmly on the surface of carrier with physical binding rather than chemical binding, thus having high enzyme activity and high stability. It has shown that the thickness of silica nano-membrane has effect on the apparent activity of Fe_3O_4@ZIF-8@CRL@SiO_2. Moreover, Fe_3O_4@ZIF-8@CRL@SiO_2 exhibits much higher stability than Fe_3O_4@ZIF-8@CRL.

Declaration of competing interest

The authors declare that they have no known competing financial interests or personal relationships that could have appeared to influence the work reported in this paper.

Acknowledgments

The authors thank the financial supports from the National Natural Science Foundation of China (Nos. 22378093, 21878065), Natural Science Foundation of Hebei Province, China (No. E2022201100), the Science and Technology Support Plan of Baoding City (No. 2241ZF111), the Medical Science Foundation of Hebei University (No. 2021A09), and the Foundation of Affiliated Hospital of Hebei University (No. 2021Z003).

Supplementary materials

Supplementary material associated with this article can be found, in the online version, at doi:10.1016/j.cclet.2024.109751.

References

[1] M. Zhang, Y. Zhang, C. Yang, C. Ma, J. Tang, Chem. Eng. J. 415 (2021) 129075.
[2] X. Zou, H. Su, F. Zhang, et al., Food Chem. 424 (2023) 136450.
[3] T.Z.P. de Figueiredo, F.A.P. Voll, N. Krieger, D.A. Mitchell, Biochem. Eng. J. 195 (2023) 108911.
[4] E.T. Hwang, S. Lee, ACS Catal. 9 (2019) 4402–4425.
[5] F. Jia, Y. Liu, X. Deng, et al., ACS Appl. Mater. Interfaces 15 (2023) 7928–7938.
[6] Q. Yang, Y. Yan, X. Yang, et al., Chem. Eng. J. 372 (2019) 946–955.
[7] R.C. Rodrigues, Á. Berenguer-Murcia, D. Carballares, R. Morellon-Sterling, R. Fernandez-Lafuente, Biotechnol. Adv. 52 (2021) 107821.
[8] G.B. Chu, W.Y. Li, X.X. Han, et al., Small 19 (2023) 2301413.
[9] R. Schoevaart, M.W. Wolbers, M. Golubovic, et al., Biotechnol. Bioeng. 87 (2004) 754–762.
[10] N. Chen, B. Chang, N. Shi, F. Lu, F. Liu, Food Chem. 399 (2023) 134000.
[11] D.M. Liu, J. Chen, Y.P. Shi, Trend Anal. Chem. 102 (2018) 332–342.
[12] S.B. Sigurdardottir, J. Lehmann, S. Ovtar, et al., Adv. Synth. Catal. 360 (2018) 2578–2607.
[13] M. Bilal, T.A. Nguyen, H.M.N. Iqbal, Coordin. Chem. Rev. 422 (2020) 213475.
[14] C. Iriarte-Mesa, M. Pretzler, C. von Baeckmann, et al., J. Colloid. Interface Sci. 646 (2023) 413–425.
[15] Y. Wang, Z. Li, W. Fu, Y. Sun, Y. Dai, Adv. Fiber. Mater. 4 (2022) 1278–1289.
[16] W. Fu, W. Xu, K. Yin, et al., Mater. Horiz. 10 (2023) 65–74.
[17] J. Han, T. Zhang, Z.Y. Zhou, H.J. Zhang, Food Chem. 417 (2023) 135810.
[18] L. Gao, J. Wen, Z. Huang, et al., ACS Appl. Mater. Interfaces 15 (2023) 31224–31232.
[19] H.A.J.A. Lawati, J. Hassanzadeh, N. Bagheri, Food Chem. 383 (2022) 132469.
[20] X. Shen, Y. Du, Z. Du, et al., Mater. Today Chem. 27 (2023) 101326.
[21] H. Cui, L. Zhang, L. Eltoukhy, et al., ACS Catal. 10 (2020) 14847–14856.
[22] Y. Weng, G. Yang, Y. Li, et al., Adv. Colloid Interface Sci. 318 (2023) 102957.
[23] G. Bayramoglu, O. Celikbicak, M. Kilic, M.Y. Arica, Food Chem. 366 (2022) 130699.
[24] L.T. Xu, K.X. Xie, S.H. Cao, et al., Chin. Chem. Lett. 34 (2023) 108181.
[25] Y.Y. Xiao, J.T. Zhang, Y.H. Dong, et al., Bioconjug. Chem. 34 (2023) 1045–1053.
[26] M.D. Gong, X.J. Pei, G.X. Duan, et al., Mater. Des. 220 (2022) 110865.
[27] S. Gadipelli, W. Travis, W. Zhou, Z. Guo, Energ. Environ. Sci. 7 (2014) 2232–2238.
[28] P. Zhang, J. Chen, B. Sun, et al., Biochem. Eng. J. 173 (2021) 108066.
[29] L. Zhong, Y. Feng, H. Hu, et al., J. Colloid Interface Sci. 602 (2021) 426–436.
[30] S. Badieyan, D.R. Bevan, C. Zhang, Biotechnol. Bioeng. 109 (2012) 31–44.
[31] J. Waeytens, J.D. Meutter, E. Goormaghtigh, A. Dazzi, V. Raussens, Anal. Chem. 95 (2023) 621–627.
[32] J.D. Meutter, E. Goormaghtigh, Anal. Chem. 93 (2021) 3733–3741.
[33] R. Lu, W.W. Li, A. Katzir, et al., Analyst 141 (2016) 6061–6067.
[34] S. Yang, Q. Zhang, H. Yang, et al., Int. J. Biol. Macromol. 206 (2022) 175–187.
[35] K.R. Webb, K.A. Hess, A. Shmidt, K.D. Segner, L.E. Buchanan, Biophys. J. 122 (2023) 1491–1502.
[36] Y.P. Cao, G.Y. Zhi, L. Han, Q. Chen, D.H. Zhang, Food Chem. 364 (2021) 130428.
[37] J. Skjold-Jørgensen, J. Vind, O.V. Moroz, et al., Biochim. Biophys. Acta Proteins Proteom. 1865 (2017) 20–27.
[38] Q. Huo, J. Zhao, W. Li, et al., Chem. Commun. 55 (2019) 7155–7158.